Author/s:
Li, J;Wasko, C;Johnson, F;Evans, JP;Sharma, A

Title:
Can Regional Climate Modeling Capture the Observed Changes in Spatial Organization of Extreme Storms at Higher Temperatures?

Date:
2018-05-16

Citation:
Li, J., Wasko, C., Johnson, F., Evans, J. P. & Sharma, A. (2018). Can Regional Climate Modeling Capture the Observed Changes in Spatial Organization of Extreme Storms at Higher Temperatures?. Geophysical Research Letters, 45 (9), pp.4475-4484. https://doi.org/10.1029/2018GL077716.

Persistent Link:
https://hdl.handle.net/11343/283974

Wasko Conrad (Orcid ID: 0000-0002-9166-8289)
Johnson Fiona (Orcid ID: 0000-0001-5708-1807)
Evans Jason, Peter (Orcid ID: 0000-0003-1776-3429)
Sharma Ashish (Orcid ID: 0000-0002-6758-0519)

Can Regional Climate Modeling capture the observed changes in spatial organization of extreme storms at higher temperatures?

J. Li[1], C. Wasko[1, 3], F. Johnson[1], J.P. Evans[2], and A. Sharma[1]

[1]School of Civil and Environmental Engineering, University of New South Wales, Sydney, New South Wales, Australia.

[2]Climate Change Research Centre and ARC Centre of Excellence for Climate Extremes, School of Biological, Environmental and Earth Sciences, University of New South Wales, Sydney, New South Wales, Australia.

[3]Department of Infrastructure Engineering, University of Melbourne, Melbourne, Victoria, Australia.

Corresponding author: Ashish Sharma (a.sharma@unsw.edu.au)

Key Points

- The spatial dependence of extreme rainfall to temperature simulated by two regional climate models is compared to observations.
- The convection-resolving model failed to simulate the positive scaling of peak precipitation for 3h storms.
- The model that adopts the Betts-Miller-Janjic convective scheme appears to best capture the observed precipitation-temperature scaling.

Abstract

The spatial extent and organization of extreme storm events has important practical implications for flood forecasting. Recently, conflicting evidence has been found on the observed changes of storm spatial extent with increasing temperatures. To further investigate this question, a Regional Climate Model assessment is presented for the Greater Sydney region, in Australia. Two RCMs were considered: the first a convection-resolving simulation

This is the author manuscript accepted for publication and has undergone full peer review but has not been through the copyediting, typesetting, pagination and proofreading process, which may lead to differences between this version and the Version of Record. Please cite this article as doi: 10.1029/2018GL077716

at 2km resolution (CRM2); the second a resolution of 10km (CPM10) with three different convection parameterizations.

Both the CRM2 and the CPM10 that used the Betts-Miller-Janjic convective scheme simulate decreasing storm spatial extent with increasing temperatures for 1h duration precipitation events, consistent with the observation-based study in Australia. However, other observed relationships of extreme rainfall with increasing temperature were not well represented by the models. Improved methods for considering storm organization are required to better understand potential future changes.

Keywords: sub-daily extreme precipitation; Clausius-Clapeyron relation; convection-resolving model; convection-parameterized model.

1 Introduction

Intensifying short-duration rainfall extremes in a warming climate have been confirmed in numerous studies based on both observations and climate model projections [*Beck et al.*, 2015; *Demaria et al.*, 2017; *Leahy and Kiely*, 2011]. This is of great concern to society as it can lead to an increased risk of flash flooding [*Westra et al.*, 2014]. These changes are generally attributed to the increased moisture holding capacity of the atmosphere at higher temperatures as governed by the Clausius-Clapeyron (CC) relationship. While the saturation water vapor pressure increases exponentially with temperature at the rate of approximately 7% per degree Celsius (see Section 3.7.3 [*Wallace and Hobbs*, 2006]), higher rates of increase (super-CC scaling) may result due to the changes of storm dynamics at warmer temperatures [*Emori and Brown*, 2005; *Loriaux et al.*, 2013; *O'Gorman*, 2012]. Based on observational records, super-CC scaling was found in the hourly rainfall extremes for temperatures between 10°C and 22°C in Netherlands, Belgium, Switzerland, Australia and Hong Kong [*Lenderink et al.*, 2011; *Lenderink and van Meijgaard*, 2008; 2010; *Wasko et al.*, 2015]. The super-CC scaling is attributed to positive feedbacks from the excess latent heat released in extreme rainfall events [*Lenderink and van Meijgaard*, 2010]. The precipitation event type also effects the scaling of sub-daily extreme storms with temperature with

different rates of scaling found for convective and stratiform events [*Berg and Haerter*, 2013; *Molnar et al.*, 2015].

While the scaling of extreme rainfall with temperature may provide some guidance on potential changes to flood producing rains due to anthropogenic climate change, it is not the entire picture. Any changes in the spatial distribution of rainfall events could act either to intensify or offset the effects of increasing storm rainfall intensities. Observations in Australia indicate that storms tend to become more concentrated around the storm center with increasing temperatures, with smaller effective radii and more spatial variability [*Wasko et al.*, 2016b]. This is consistent with model studies using the Weather Forecasting and Research model with the Grell-Devenyi convective parameterization (Wang and Kotamarthi, 2015) where decreases in storm size regardless of season were predicted [*Chang et al.*, 2016]; and decreases in storm cell size using a downscaled GCM and a stochastic weather generator [*Bordoy and Burlando*, 2014]. Additionally, extratropical cyclones under climate warming have been predicted to become more concentrated and intense [*Pfahl et al.*, 2015; *Shi and Durran*, 2016]. However, there is also evidence that storm areas may be larger at higher temperatures [*Lenderink et al.*, 2017; *Lochbihler et al.*, 2017], highlighting the urgent need for more research in this area to resolve these conflicting findings.

One way of providing further insight into this issue is through climate modelling studies. Global climate models (GCMs) typically run at a coarse resolution of 100-300km and are unable to resolve the physical processes related to short-duration extreme rainfall. Regional climate models (RCMs) provide a better representation of localized processes including some skill in the representing the temperature dependence of extreme rainfall [*Singleton and Toumi*, 2013]. However, there are still concerns with the ability of RCMs to represent the timing of extreme storms caused by deep convection [*Cortés-Hernández et al.*, 2016]. A further problem is the suppressed variability in temperature scaling of rainfall compared to observations. The convection parameterization schemes in RCMs lead to these problems, because they misrepresent the local-scale physical processes that drive deep convection and contribute to short-duration extreme rainfall.

These problems have been addressed using convection-resolving (i.e. horizontal resolution less than 4km) models (CRMs) [*Kendon et al.*, 2017]. Such models have shown added value in producing sub-daily rainfall characteristics with improved representation of diurnal cycle of local-scale convection [*Argüeso et al.*, 2016] and occurrence of hourly heavy rainfall events [*Ban et al.*, 2014]. Model and observed scaling rates of precipitation extremes with temperature have also been found to be similar [*Bao et al.*, 2017]. However, the temperature scaling of the spatial distribution of extreme rainfall events from these models has not yet been investigated. We investigate the temperature and spatial rainfall scaling relationships from a 2km convection-resolving model (CRM2) and compare these to the relationships from observations and a 10km convection-parametrization model (CPM10) over the Greater Sydney region.

2 Data and method

2.1 Observations

This study used the same sub-daily observational records as in *Wasko et al.* [2016b] restricted to the Greater Sydney region to match the domain of the RCMs. Six-minute precipitation and three-hourly 1.2m dry-bulb temperatures were provided by the Australian Bureau of Meteorology for 53 gauges (Figure 1a). The temporal coverage of the observations varies with gauges. To maximize the data length used for analysis, the full record at each gauge was used. The six-minute observational rainfall was aggregated to hourly time scale to match the temporal resolution of the model simulations.

2.2 Regional climate model simulations

The 10km convection-parameterization model (CPM10) and the 2km convection-resolving model (CRM2) chosen for this study are part of the NSW/ACT Regional Climate Modelling (NARCliM) project [*Evans and Argüeso*, 2015; *Evans et al.*, 2014] and used the Weather Research and Forecasting (WRF) model version 3.3 [*Skamarock et al.*, 2008]. The CPM10 has output at hourly resolution using three different physical schemes (Table 1) from 1950 to 2010. The CPM10 model is nested inside the 50km simulation that is driven by the six-hourly

boundary conditions extracted from the NCEP-NCAR reanalysis project (NNRP). The detailed model design can be found in *Evans et al.* [2014] and extensive evaluation of the simulations has found a good representation of precipitation and temperature fields [*Olson et al.*, 2016] including extremes [*Cortés-Hernández et al.*, 2016; *Evans et al.*, 2017], and climate mode teleconnections [*Fita et al.*, 2017]. Apart from the aforementioned 3 NNRP-driven CPM10 ensembles, the three 10km RCMs have another 12 simulations with boundary conditions derived from 4 different GCMs. As the reanalysis dataset is considered to better represent the observations than GCM simulations, the reanalysis-driven RCM will provide a better assessment of model skill compared to observations than the GCM-driven RCM. As such, this study only used the NNRP-driven CPM10 simulations. The CRM2 is double nested within the 50km and 10km WRF simulations and covers the period from 1990-2009. The CPM10 simulations cover south-east Australia, whereas the CRM2 is only available over the study domain of the Greater Sydney region (Figure 1). The CRM2 simulation has also been evaluated against observations demonstrating good performance for temperature [*Argüeso et al.*, 2014] and spatially varying biases for precipitation [*Evans and Argüeso*, 2015]. The CRM2 simulation has previously been used to investigate the climate change impact on areal reduction factors [*Li et al.*, 2015] and design rainfall [*Li et al.*, 2017]. Hourly precipitation and surface air temperature simulated by the CRM2 and the three ensemble members of the CPM10 were used. To ensure that the results from gridded simulations and point observations are comparable, only the nearest grid-cells corresponding to the 53 sub-daily gauges were used in analysis. The time period used for the spatial field analysis is 1990-2009 for both RCMs. Table S1 summarizes the statistics of temperature and precipitation at Sydney Observatory Hill (151.2050°E, -33.8607°S) for the observations and model simulations. All four model runs simulated the temperature statistics and the mean precipitation well. The models underestimate the 90^{th} percentile rainfall with the CRM2 model providing the best match to the observations. The maximum rainfall simulated by the models is quite variable compared to observations. Given that the resolution of the CPM10 models is 10 km some moderation of the extremes is expected, which is consistent with typical Areal Reduction

Factors. The overestimation of the maximum rainfall by CRM2 is consistent with the findings of *Evans and Argüeso* [2015].

2.3 Method

The aim of the analyses is to investigate the spatial organization of moisture within a storm following the method of Wasko et al. [2016b]. The data used in analyses for both the observations and RCM simulations are from the 53 sub-daily gauges locations. The method used for the observations is also applicable to the RCM simulations. The process starts by identifying independent 1h and 3h storms in the hourly precipitation time series using a minimum inter-event dry period of 5 hours and 15 hours, respectively [Wasko and Sharma, 2014]. The maximum 1h and 3h precipitation burst within each storm was paired with the 24h temperature average centered on the time of the maximum precipitation. The 24h temperature average was chosen to remove the effects of the diurnal circle [*Rasuly*, 1996]. The precipitation-temperature pairs were then extended to form spatial fields. Potential spatial fields consist of all neighboring grid points with precipitation at the same time within a radius of 50km. The spatial fields are then screened to ensure that the maximum precipitation occurs at the center and that they have at least four neighboring stations with rainfall. Spatial fields that did not meet these criteria were not used in the analyses. Therefore, by definition the maximum precipitation occurs at the center of the spatial field.

Extreme events were then identified through exponential quantile regression. Only the spatial fields with maximum precipitation greater than the 90^{th} percentile were used to represent the spatial distribution of moisture. Quantile regression was used to extract the extreme events instead of binning because it is unbiased with sample size and it does not make any assumption on bin size, or subjectively exclude data that falls into the bins with small sample size [*Morrison and Spencer*, 2014; *Wasko and Sharma*, 2014]. The 90^{th} percentile was chosen here to extract the extreme events so that the results are comparable with those presented in *Wasko et al.* [2016b]. We also attempted to use the 95^{th} percentile as the threshold to separate the extreme and non-extreme events. However, there are not enough points above the 95^{th} percentile line to fit a robust exponential curve at some locations.

For the extreme spatial fields, the following statistics were calculated:

1. Peak precipitation (PP), which is the maximum precipitation at the original central gauge location of the spatial field.
2. Total precipitation (PT), estimated as the two-dimensional integration of the precipitation plotted against the distance from the storm center.
3. Effective radius (RE), defined as the centroid of the storm where p_{ij} is the i^{th} precipitation observation within the spatial field j at a distance of d_{ij} from the center.

$$RE_j = \frac{\sum_{i=1}^{n} p_{ij} d_{ij}}{\sum_{i=1}^{n} p_{ij}}$$

4. Coefficient of variation (CV), defined as the ratio of the standard deviation of the precipitation in the spatial field to the mean.
5. Fraction of zero precipitation observations (PZ) within the spatial field.

Consistent with *Wasko et al.* [2016b] an exponential regression was fitted for the first four statistics against temperature and a linear regression was used to examine the relationship between the fraction of zero precipitation and temperature. As the statistics described above were estimated for the spatial field rather than a single point, the relationship between those statistics and temperature was also calculated for the spatial field.

3 Results

To examine the quality of the scaling estimation, the fitted exponential regression of the selected statistic scaling for 1h storms using the precipitation simulated by the CRM2 is shown in Figure S1 for a randomly selected location. Increases in the peak precipitation, the total precipitation and the coefficient of variation were found, whereas decreases were found in the effective radius. The scaling relationships are reasonably consistent across the range of temperatures modelled during the study period.

Figure 2 presents the scaling of peak precipitation with temperature for 1h storms. The three ensemble members of CPM10 have similar positive scaling of peak precipitation to the

observations. However, CRM2 underestimated the positive scaling and even simulated negative scaling along the coastal fringe, although these estimates are not statistically significant at the 5% level. Positive scaling of peak precipitation was also found for 3h storms with significant negative scaling estimated using the CRM2 simulations (Figure S2). Despite the improved skill in resolving the mechanisms that lead to localized short duration extreme rainfall, the biases in the extreme precipitation simulated by the model [*Jakob et al.*, 2015] mean that the scaling relationships are not as well represented as in the convection-parameterization model. Similar results were found for 1h total precipitation (Figure S3) such that CRM2 showed negative scaling whilst positive scaling was found in the observations. While all three ensemble members of CPM10 captured the positive scaling of the total precipitation, CPM10-R1 and CPM10-R3 slightly overestimated the magnitude of the scaling at a few sites. A better match between CRM2 and observations of total precipitation scaling was found for the 3h events, including for both negative and positive scaling locations, whilst for this duration none of the CPM10 simulations indicated negative scaling. The divergence in the scaling of peak precipitation between observation and the CRM2 is likely to be caused by the unrealistic simulation of 1h maximum precipitation burst exceeding the 90^{th} percentile quantile regression curve as shown in Figure S5. The over-simulation of maximum precipitation has been noted before for this model [*Evans and Argüeso,* 2015]. Unlike other statistics examined here, the peak precipitation scaling is more sensitive to the values at a single point location. Therefore, it is not surprising to see some divergence in the peak precipitation scaling between observations and the CRM2. As the CRM2 was double nested inside the 50km and 10km WRF simulations, this finding suggests that it is more difficult to maintain the consistency between temperature and extreme precipitation at a finer scale.

Moving to the spatial distribution of extreme rainfall events (Figure 3) both the CRM2 and CPM10-R2 confirm the negative scaling of storm effective radius found by *Wasko et al.* [2016b]. The magnitude of the scaling in the models is slightly smaller than in the observations for both the 1h and 3h storms (Figure S6). The two CPM10 models using the Kain-Fritsch scheme had markedly different RE scaling compared to the observations and the other two models. It is known that the Kain-Fritsch scheme tends to leave unrealistically deep

saturated layers in post-convective sounding, thus activating the microphysics scheme to simulate too much stratiform precipitation [*Fiori et al.*, 2014] and possibly resulting in increases in the storm size with higher temperatures.

The positive scaling of peak and total precipitation and the negative scaling of effective radius estimated from observations suggest that extreme storms are likely to become more concentrated at the storm centers at warmer temperatures. This behavior was also reflected in the CPM10-R2 and CRM2 simulations for 1h duration storms, consistent with the conclusions of *Wasko et al.* [2016b]. Two other statistics of storm spatial scaling were calculated, namely the coefficient of variability (CV) and the fraction of zero precipitation. Observations show more variability within a storm (higher CV) with increasing temperatures (Figure S7) and more zero precipitation locations (Figure 4).

Increasing variability in the storm rainfall totals was simulated by all models (Figure S7) although CRM2, CPM10-R1 and CPM10-R3 simulated non-significant negative scaling for the few sites along the east coast. The observed positive scaling of the fraction of zero precipitation was not seen in any of the model simulations (Figure 4), which is not surprising due to the widely reported drizzling effect in RCM simulations [*Argüeso et al.*, 2013; *Olsson et al.*, 2015; *Teutschbein and Seibert*, 2013]. The results for 3h storms (Figure S8 and S9) are similar to those estimated for 1h storms.

Figure 5 summarizes the scaling for all statistics estimated from the observations, the CRM2 and the three ensemble members of the CPM10 for 1h storms. For all statistics, the model estimates of scaling are damped compared to the observations, with this effect much stronger in the convection resolving RCM. Figure 5 also highlights that the direction of scaling estimated by the models is generally consistent with the observations, with the exception of the effective radius. Different cumulus convection schemes lead to quite different conclusions on the relationship of storm area with temperature. Based on the method for defining storm size used here the Betts-Miller-Janjic cumulus convection scheme is able to simulate the observed spatial redistribution of moisture within a storm at higher temperatures as can the CRM2. Considering all the five sets of statistics, the CPM10-R2 best captures the observed changes in spatial organization of extreme storms as temperature increases.

Due to the scarcity of sub-daily precipitation observations, the longest record available at each of the 53 rain gauges was used. This leads to varying temporal coverage for observational analysis at different locations. In contrast, a fixed time period (i.e. 1990-2009) was chosen for the analysis using model simulations. A sensitivity test was performed using the same analyses periods for a small subset of the stations and the conclusions were consistent with those presented above.

4 Discussion and conclusions

This study was motivated by conflicting findings on the influence of temperature on storm sizes [*Lochbihler et al.*, 2017; *Wasko et al.*, 2016b]. Regional climate model simulations can provide further lines of evidence on the relationship between storm events and increasing temperatures. Two of the RCM simulations confirm the results of *Wasko et al.* [2016b] with the effective radius of storms decreasing with increasing temperature. The RCM simulations using the Kain-Fritsch scheme lead to the opposite conclusion, however, the known weaknesses in this scheme with respect to the proportion of stratiform rainfall lead to less confidence in this finding.

The studies of changing spatial storm characteristics have used very different methods for characterizing the size, shape and properties of storm events as well as being implemented in parts of the world with quite different climates. For example, *Wasko et al.* [2016b] used gauge data for Australia, *Lochbihler et al.* [2017] used radar data for the Netherlands, while other studies used models of varying resolution for North America [*Chang et al.*, 2016; *Guinard et al.*, 2015]. For consistency with *Wasko et al.* [2016b], in this study, precipitation and temperature data was extracted from the RCM simulations only at the locations where rain gauges are available. The analysis also assumes an Eulerian frame of reference and does not account for storm advection. This is necessary due to the limited number of pluviograph stations within the study area. Using a Lagrangian frame of reference which tracks the storm cell may or may not produce different scaling results [*Chang et al.*, 2016; *Lochbihler et al.*, 2017]. Using a storm tracking algorithm may enable a more extensive use of the RCM simulations across the full model domain, and enable relaxing of the implicit assumption of

circular storms, but then a direct evaluation of the RCM with observations would not have been possible. Any rainfall that occurred concurrently within a 50km radius is considered as part of the same storm event. This distance was chosen to ensure that a sufficient number of neighboring gauge stations are included in the analysis. The choice of radius is a tradeoff between missing some parts of large storms and enclosing several different local storms that occurred at the same time. However, because the analyses were restricted to locations with a large number of spatial fields (i.e. a minimum of 100 spatial fields) the results are considered representative of the overall characteristics of a majority of extreme storms.

In addition to the choice of radius, the underlying distribution of the rain gauge network also affects the estimation of extreme spatial field statistics to some extent. As shown in Figure 1, the spatial distribution of the rain gauges is not uniform with low station densities in the north west of the study area due to the topography, vegetation and low population in this area. As this study used a subset of RCM outputs at the rain gauge locations, the spatial field membership is the same between the RCM and the station-based analysis, the comparison of results is fair. However, future work is recommended to use the full RCM grid to allow the spatial fields to be defined consistently across the study domain and not be affected by the rain gauge density.

The use of climate model simulations to assess scaling introduces two other issues that may affect the conclusions. The rainfall estimates from each model grid are assumed to be representative of the point extreme value measured at a rain gauge of the same location. It is known that area-averaged extreme precipitation is often lower than the point value since it is unlikely that the extreme precipitation occurs concurrently at multiple points within a defined area [*Li et al.*, 2015]. This issue is more important for the CPM10 simulations which have grid cell areas of approximately 100 km^2. *Li et al.* [2015] showed for the same 2km resolution CRM the grid resolution is small enough to approximate the point rainfall. The scale mismatch between grid simulations and point observations may lead to biased estimates of precipitation-temperature relation. However, similar analysis performed on remotely sensed rainfall demonstrates that the scaling relations do hold on gridded products [*Wasko et al.*, 2016a] providing confidence in using climate model simulations to further explore scaling.

The second issue with the use of climate models is the bias in the simulation of precipitation. Here the simulations have not been bias corrected, assuming that the biases in the model are constant across all temperatures. *Li et al.* [2016] assessed biases in different storm types in these RCMs for daily precipitation. No significant changes in the bias and proportion of storms in the future were found, however further work is required to extend this analysis to the sub-daily simulations considered here. This is particularly important because the mechanisms explaining departures from the thermodynamic scaling rates (Clausius-Clapeyron) include changes to storm dynamics [*Lenderink and van Meijgaard*, 2010] and mixing of storm event type [*Berg and Haerter*, 2013; *Molnar et al.*, 2015]. Therefore, if there are biases in different storm types in the climate model simulations and the storm types themselves vary with temperature, the climate model biases may influence the estimated scaling rates. However, the reasonable matches between the precipitation intensity scaling with observations found here suggest that this may not be a significant issue in these models.

Another concern is the effect of urban land use on the relationships between temperature and extreme precipitation. While the models adopted the land use data derived from satellite based global datasets, representing the early 1990s, the actual urban area has increased from 1990 to 2009. However, since all the stations used in the analysis have had limited changes in their surrounding urbanisation, the urban expansion is expected to have negligible effect on the analysis used here.

The results here suggest that as temperatures increase, short duration storm events will become more intense over smaller areas, which has important implications for hydrologic engineering design and flood management. Because this study used two different convective parametrizations and a RCM run at a resolution that allows for convection to be fully resolved, it highlights better modelling methodologies to represent observed extreme precipitation scaling relationships. Modelling studies have indicated that future precipitation scaling rates may exceed those found in the historical record [*Bao et al.*, 2017]. Future work should consider whether this also applies to the scaling of storm spatial properties found here. The results show that both the convection resolving model and convection parameterized model are capable of simulating the intensification of peak precipitation and total

precipitation for 1h storms as temperature increases, which indicates that the thermodynamic mechanism of increasing moisture capacity causing increased precipitation is properly modelled by both RCMs at hourly time scale. The positive scaling of peak and total precipitation and the negative scaling of effective radius reflect that at higher temperatures moisture is likely to redistribute from the storm boundaries to the storm center. This pattern was best captured by the convection-parameterized model that uses the Betts-Miller-Janjic cumulus convection scheme and the convection-resolving model for 1h storms, although the latter slightly underestimated the increased heterogeneity of the precipitation at higher temperatures. In addition, the convection-resolving model simulated weakened peak precipitation intensity for 3h storms at higher temperatures, which is contradictory to the observations. In this case, the convection-resolving model did not provide a better simulation of the relationship between temperature and extreme precipitation, which suggest that a better representation of convection does not always translate to a better simulation of precipitation. Precipitation simulation is also affected by other model parameterizations such as the cloud microphysics and planetary boundary layer. Sensitives related to the cloud microphysics and the cloud-radiative feedback are considerably larger than those related to mesh refinement at kilometer scales (Prein et al., 2015). The scaling results presented here provide one way of evaluating the performance of RCMs and we find that somewhat counterintuitively the convection-resolving model used here does not always outperform its convection-parameterized counterpart for this statistic.

Acknowledgments

Regional climate data have been provided by the New South Wales and Australian Capital Territory Regional Climate Model (NARCliM) project funded by NSW Governmental Office of Environment and Heritage, University of New South Wales Climate Change Research Centre (CCRC), ACT Government Environment and Sustainable Development Directorate and other project partners. The RCM data is available at http://climatechange.environment.nsw.gov.au/Climate-projections-for-NSW/Download-datasets. The rainfall data can be obtained from http://www.bom.gov.au/climate/data/stations/. This work was made possible by funding from

the Australian Research Council as part of DP120100338 and FT110100576. This work was supported by an award under the Merit Allocation Scheme on the NCI National Facility at the ANU. F. Johnson and J. Li were supported through ARC Discovery Project DP150100411. This research/project was undertaken with the assistance of resources and services from the National Computational Infrastructure (NCI), which is supported by the Australian Government.

References

Argüeso, D., A. Di Luca, and J. P. Evans (2016), Precipitation over urban areas in the western Maritime Continent using a convection-permitting model, *Climate dynamics*, *47*(3-4), 1143-1159.

Argüeso, D., J. P. Evans, and L. Fita (2013), Precipitation bias correction of very high resolution regional climate models, *Hydrol. Earth Syst. Sci.*, *17*(11), 4379-4388, doi:10.5194/hess-17-4379-2013.

Argüeso, D., J. P. Evans, L. Fita, and K. J. Bormann (2014), Temperature response to future urbanization and climate change, *Climate Dynamics*, 1-17, doi:10.1007/s00382-013-1789-6.

Ban, N., J. Schmidli, and C. Schär (2014), Evaluation of the convection-resolving regional climate modeling approach in decade-long simulations, *Journal of Geophysical Research: Atmospheres*, *119*(13), 7889-7907, doi:10.1002/2014JD021478.

Bao, J., S. C. Sherwood, L. V. Alexander, and J. P. Evans (2017), Future increases in extreme precipitation exceed observed scaling rates, *Nature Clim. Change*, *7*(2), 128-132, doi:10.1038/nclimate3201

http://www.nature.com/nclimate/journal/v7/n2/abs/nclimate3201.html - supplementary-information.

Beck, F., A. Bárdossy, J. Seidel, T. Müller, E. Fernandez Sanchis, and A. Hauser (2015), Statistical analysis of sub-daily precipitation extremes in Singapore, *Journal of Hydrology: Regional Studies*, *3*, 337-358, doi:http://dx.doi.org/10.1016/j.ejrh.2015.02.001.

Berg, P., and J. O. Haerter (2013), Unexpected increase in precipitation intensity with temperature — A result of mixing of precipitation types?, *Atmospheric Research*, *119*(0), 56-61, doi:http://dx.doi.org/10.1016/j.atmosres.2011.05.012.

Bordoy, R., and P. Burlando (2014), Stochastic downscaling of climate model precipitation outputs in orographically complex regions: 2. Downscaling methodology, *Water Resources Research*, *50*(1), 562-579, doi:10.1002/wrcr.20443.

Chang, W., M. L. Stein, J. Wang, V. R. Kotamarthi, and E. J. Moyer (2016), Changes in Spatiotemporal Precipitation Patterns in Changing Climate Conditions, *Journal of Climate*, *29*(23), 8355-8376, doi:10.1175/jcli-d-15-0844.1.

Cortés-Hernández, V. E., F. Zheng, J. P. Evans, M. Lambert, A. Sharma, and S. Westra (2016), Evaluating regional climate models for simulating sub-daily rainfall extremes, *Climate Dynamics*, *47*(5), 1613-1628, doi:10.1007/s00382-015-2923-4.

Demaria, E., D. Goodrich, and T. Keefer (2017), *Frequency Analysis of Extreme Sub-Daily Precipitation under Stationary and Non-Stationary Conditions across Two Contrasting Hydroclimatic Environments*, 1-28 pp., doi:10.5194/hess-2017-247.

Emori, S., and S. J. Brown (2005), Dynamic and thermodynamic changes in mean and extreme precipitation under changed climate, *Geophysical Research Letters*, *32*(17), n/a-n/a, doi:10.1029/2005GL023272.
Evans, J. P., and D. Argüeso (2015), 'WRF simulations of future changes in rainfall IFD curves over Greater Sydney', in *the Art and Science of Water - 36th Hydrology and Water Resources Symposium*, Engineers Australia: 33-38.
https://search.informit.com.au/documentSummary;dn=814656266329832;res=IELENG
Evans, J. P., D. Argueso, R. Olson, and A. Di Luca (2017), Bias-corrected regional climate projections of extreme rainfall in south-east Australia, *Theoretical and Applied Climatology*, *130*(3), 1085-1098, doi:10.1007/s00704-016-1949-9.
Evans, J. P., F. Ji, C. Lee, P. Smith, D. Argüeso, and L. Fita (2014), Design of a regional climate modelling projection ensemble experiment–NARCliM, *Geoscientific Model Development*, *7*(2), 621-629.
Fiori, E., A. Comellas, L. Molini, N. Rebora, F. Siccardi, D. J. Gochis, S. Tanelli, and A. Parodi (2014), Analysis and hindcast simulations of an extreme rainfall event in the Mediterranean area: The Genoa 2011 case, *Atmospheric Research*, *138*, 13-29, doi:http://dx.doi.org/10.1016/j.atmosres.2013.10.007.
Fita, L., J. P. Evans, D. Argüeso, A. King, and Y. Liu (2017), Evaluation of the regional climate response in Australia to large-scale climate modes in the historical NARCliM simulations, *Climate Dynamics*, *49*(7), 2815-2829, doi:10.1007/s00382-016-3484-x.
Guinard, K., A. Mailhot, and D. Caya (2015), Projected changes in characteristics of precipitation spatial structures over North America, *International Journal of Climatology*, *35*(4), 596-612, doi:10.1002/joc.4006.
Jakob, D., A. Griesser, and A. Seed (2015), Assessing the credibility of downscaled rainfall extremes for the Greater Sydney region–a novel approach using blended radar/gauge data, paper presented at 36th Hydrology and Water Resources Symposium: The art and science of water, Engineers Australia.
Kendon, E. J., N. Ban, N. M. Roberts, H. J. Fowler, M. J. Roberts, S. C. Chan, J. P. Evans, G. Fosser, and J. M. Wilkinson (2017), Do Convection-Permitting Regional Climate Models Improve Projections of Future Precipitation Change?, *Bulletin of the American Meteorological Society*, *98*(1), 79-93, doi:10.1175/bams-d-15-0004.1.
Leahy, P. G., and G. Kiely (2011), Short Duration Rainfall Extremes in Ireland: Influence of Climatic Variability, *Water Resour Manage*, *25*(3), 987-1003, doi:10.1007/s11269-010-9737-2.
Lenderink, G., R. Barbero, J. M. Loriaux, and H. J. Fowler (2017), Super-Clausius–Clapeyron Scaling of Extreme Hourly Convective Precipitation and Its Relation to Large-Scale Atmospheric Conditions, *Journal of Climate*, *30*(15), 6037-6052, doi:10.1175/jcli-d-16-0808.1.
Lenderink, G., H. Y. Mok, T. C. Lee, and G. J. Van Oldenborgh (2011), Scaling and trends of hourly precipitation extremes in two different climate zones–Hong Kong and the Netherlands, *Hydrology and Earth System Sciences*, *15*(9), 3033-3041.
Lenderink, G., and E. van Meijgaard (2008), Increase in hourly precipitation extremes beyond expectations from temperature changes, *Nature Geosci*, *1*(8), 511-514, doi:doi: 10.1038/ngeo262.
Lenderink, G., and E. van Meijgaard (2010), Linking increases in hourly precipitation extremes to atmospheric temperature and moisture changes, *Environmental Research Letters*, *5*(2), 025208.

Li, J., J. P. Evans, F. Johnson, and A. Sharma (2017), A comparison of methods for estimating climate change impact on design rainfall using a high-resolution RCM, *Journal of Hydrology*, *547*, 413-427, doi:https://doi.org/10.1016/j.jhydrol.2017.02.019.
Li, J., A. Sharma, J. Evans, and F. Johnson (2016), Addressing the mischaracterization of extreme rainfall in regional climate model simulations–A synoptic pattern based bias correction approach, *Journal of Hydrology*, doi:10.1016/j.jhydrol.2016.04.070.
Li, J., A. Sharma, F. Johnson, and J. P. Evans (2015), Evaluating the effect of climate change on areal reduction factors using regional climate model projections, *Journal of Hydrology*, *528*, 419-434, doi:http://dx.doi.org/10.1016/j.jhydrol.2015.06.067.
Lochbihler, K., G. Lenderink, and A. P. Siebesma (2017), The spatial extent of rainfall events and its relation to precipitation scaling, *Geophysical Research Letters*, n/a-n/a, doi:10.1002/2017GL074857.
Loriaux, J. M., G. Lenderink, S. R. D. Roode, and A. P. Siebesma (2013), Understanding Convective Extreme Precipitation Scaling Using Observations and an Entraining Plume Model, *Journal of the Atmospheric Sciences*, *70*(11), 3641-3655, doi:10.1175/jas-d-12-0317.1.
Molnar, P., S. Fatichi, L. Gaál, J. Szolgay, and P. Burlando (2015), Storm type effects on super Clausius–Clapeyron scaling of intense rainstorm properties with air temperature, *Hydrol. Earth Syst. Sci.*, *19*(4), 1753-1766, doi:10.5194/hess-19-1753-2015.
Morrison, T., and P. Spencer (2014), Quantile Regression-A Statisticians Approach to the Local Ice Pressure-Area Relationship, paper presented at OTC Arctic Technology Conference, Offshore Technology Conference.
Nicolet, G., N. Eckert, S. Morin, and J. Blanchet (2016), Decreasing spatial dependence in extreme snowfall in the French Alps since 1958 under climate change, *Journal of Geophysical Research: Atmospheres*, *121*(14), 8297-8310, doi:10.1002/2016JD025427.
O'Gorman, P. A. (2012), Sensitivity of tropical precipitation extremes to climate change, *Nature Geosci*, *5*(10), 697-700, doi:http://www.nature.com/ngeo/journal/v5/n10/abs/ngeo1568.html - supplementary-information.
Olson, R., J. P. Evans, A. Di Luca, and D. Argueso (2016), The NARCliM project: Model agreement and significance of climate projections, *Clim. Res*, *69*, 209-227.
Olsson, J., P. Berg, and A. Kawamura (2015), Impact of RCM Spatial Resolution on the Reproduction of Local, Subdaily Precipitation, *Journal of Hydrometeorology*, *16*(2), 534-547, doi:10.1175/jhm-d-14-0007.1.
Pfahl, S., P. A. O'Gorman, and M. S. Singh (2015), Extratropical Cyclones in Idealized Simulations of Changed Climates, *Journal of Climate*, *28*(23), 9373-9392, doi:10.1175/jcli-d-14-00816.1.
Rasuly, A. A. (1996), Temporal and spatial study of thunderstorm rainfall in the Greater Sydney region, Doctor of Philosophy Thesis, School of Geosciences, University of Wollongong, http://ro.uow.edu.au/theses/1986/
Prein, A. F., W. Langhans, G. Fosser, A. Ferrone, N. Ban, K. Goergen, M. Keller, M. Tölle, O. Gutjahr, F. Feser, et al. (2015), A review on regional convection-permitting climate modeling: Demonstrations, prospects, and challenges, *Rev. Geophys.*, 53, 323–361. doi:10.1002/2014RG000475.
Shi, X., and D. Durran (2016), Sensitivities of Extreme Precipitation to Global Warming Are Lower over Mountains than over Oceans and Plains, *Journal of Climate*, *29*(13), 4779-4791, doi:10.1175/jcli-d-15-0576.1.
Singleton, A., and R. Toumi (2013), Super-Clausius–Clapeyron scaling of rainfall in a model squall line, *Quarterly Journal of the Royal Meteorological Society*, *139*(671), 334-339, doi:10.1002/qj.1919.

Skamarock, W. C., J. B. Klemp, J. Dudhia, D. O. Gill, D. M. Barker, M. G. Duda, X. Huang, W. Wang, and J. G. Powers (2008), A description of the advanced research WRF version 3*Rep.*, 7-25 pp.
Teutschbein, C., and J. Seibert (2013), Is bias correction of regional climate model (RCM) simulations possible for non-stationary conditions?, *Hydrol. Earth Syst. Sci.*, *17*(12), 5061-5077, doi:10.5194/hess-17-5061-2013.
Wallace, J. M., and P. V. Hobbs (2006), *Atmospheric science: an introductory survey*, Academic press.
Wasko, C., R. M. Parinussa, and A. Sharma (2016a), A quasi-global assessment of changes in remotely sensed rainfall extremes with temperature, *Geophysical Research Letters*, *43*(24), 12,659-612,668, doi:10.1002/2016GL071354.
Wang, J., and V. R. Kotamarthi (2015): High-resolution dynamically downscaled projections of precipitation in the mid and late 21st century over North America. *Earth's Future*, **3**, 268–288, doi:https://doi.org/10.1002/2015EF000304.
Wasko, C., and A. Sharma (2014), Quantile regression for investigating scaling of extreme precipitation with temperature, *Water Resources Research*, *50*(4), 3608-3614, doi:10.1002/2013WR015194.
Wasko, C., A. Sharma, and F. Johnson (2015), Does storm duration modulate the extreme precipitation-temperature scaling relationship?, *Geophysical Research Letters*, *42*(20), 8783-8790, doi:10.1002/2015GL066274.
Wasko, C., A. Sharma, and S. Westra (2016b), Reduced spatial extent of extreme storms at higher temperatures, *Geophysical Research Letters*, *43*(8), 4026-4032, doi:10.1002/2016GL068509.
Westra, S., H. J. Fowler, J. P. Evans, L. V. Alexander, P. Berg, F. Johnson, E. J. Kendon, G. Lenderink, and N. M. Roberts (2014), Future changes to the intensity and frequency of short-duration extreme rainfall, *Reviews of Geophysics*, *52*(3), 522-555, doi:10.1002/2014RG000464.

Figure 1. Greater Sydney region with the locations of sub-daily rain gauges indicated by the red dots (left) and the domains for the 10km and 2km RCMs (right).

Figure 2. Scaling of the peak precipitation (PP) with temperature for 1h storms. The size of the circles is proportional to the magnitude of the scaling. The sign of the scaling is indicated by the color with blue representing negative scaling and red positive scaling. The cross marker indicates the scaling is statistically significant at 5% level.

Figure 3. Scaling of the effective radius (RE) with temperature for 1h storms.

Figure 4. Scaling of fraction of zero precipitation (PZ) with temperature for 1h storms.

Figure 5. Box plots of peak precipitation (PP) scaling, effective radius (RE) scaling, total precipitation (PT) scaling, fraction of zero precipitation (PZ) scaling, and coefficient of variation (CV) scaling for 1h storms.

Table 1. Physical schemes of the three ensembles of the 10km-resolution convection-parameterization model (CPM10).

CPM10 ensemble	Planetary boundary layer scheme	Cumulus convection	Cloud microphysics scheme	Shortwave/Longwave radiation physics scheme

run		scheme		
R1	Mellor-Yamada-Janjic/Eta similarity	Kain-Fritsch	WRF Double Moment 5-class	Dudhia/Rapid Radiative Transfer Model
R2	Mellor-Yamada-Janjic/Eta similarity	Betts-Miller-Janjic	WRF Double Moment 5-class	Dudhia/Rapid Radiative Transfer Model
R3	Yonsei University/MM5 similarity	Kain-Fritsch	WRF Double Moment 5-class	NCAR Community Atmosphere

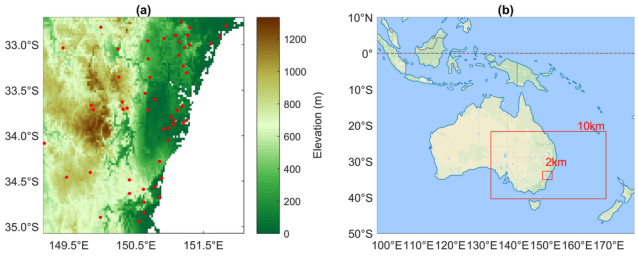

2018GL077716-f01-z-.tif

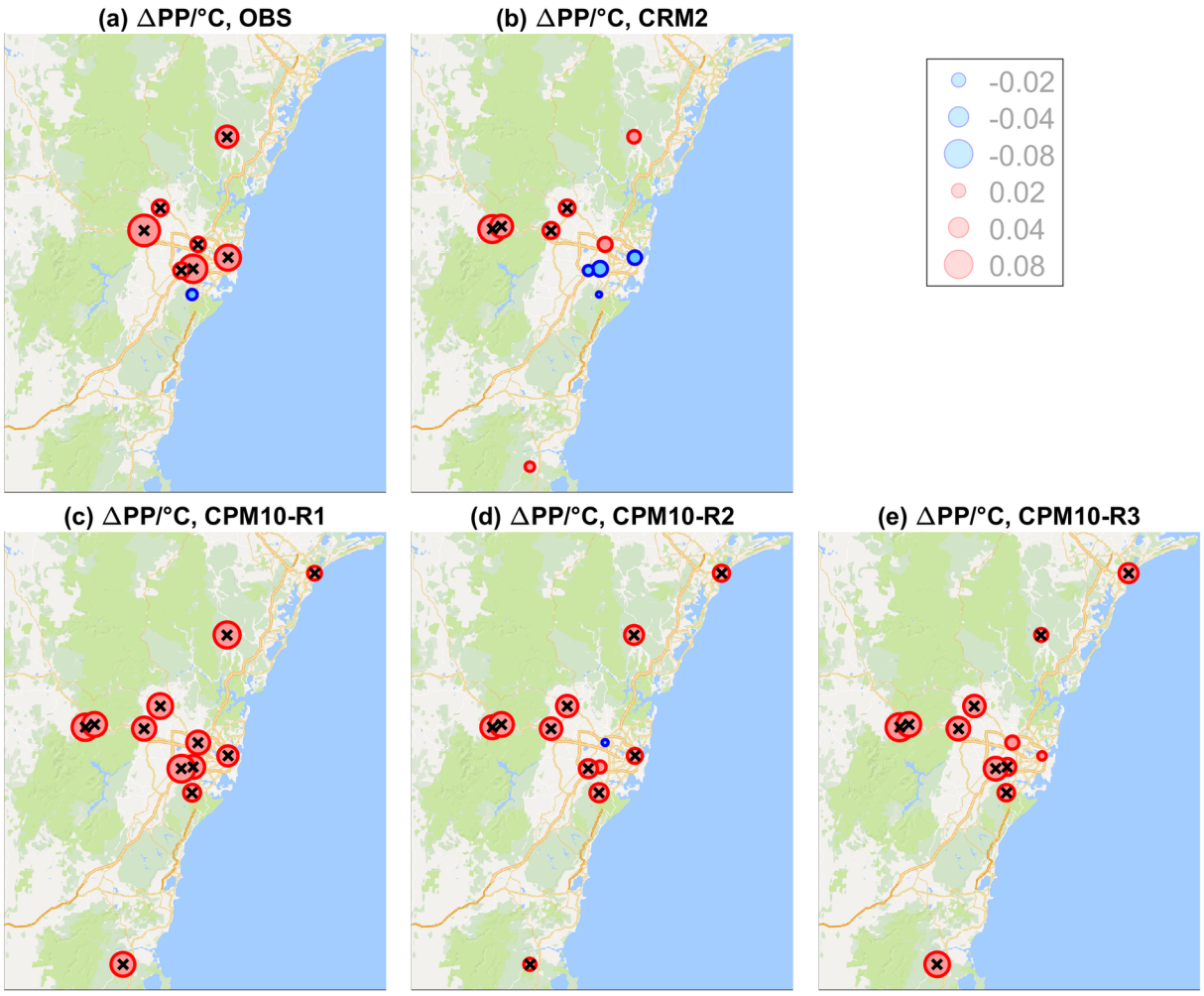

2018GL077716-f02-z-.tif

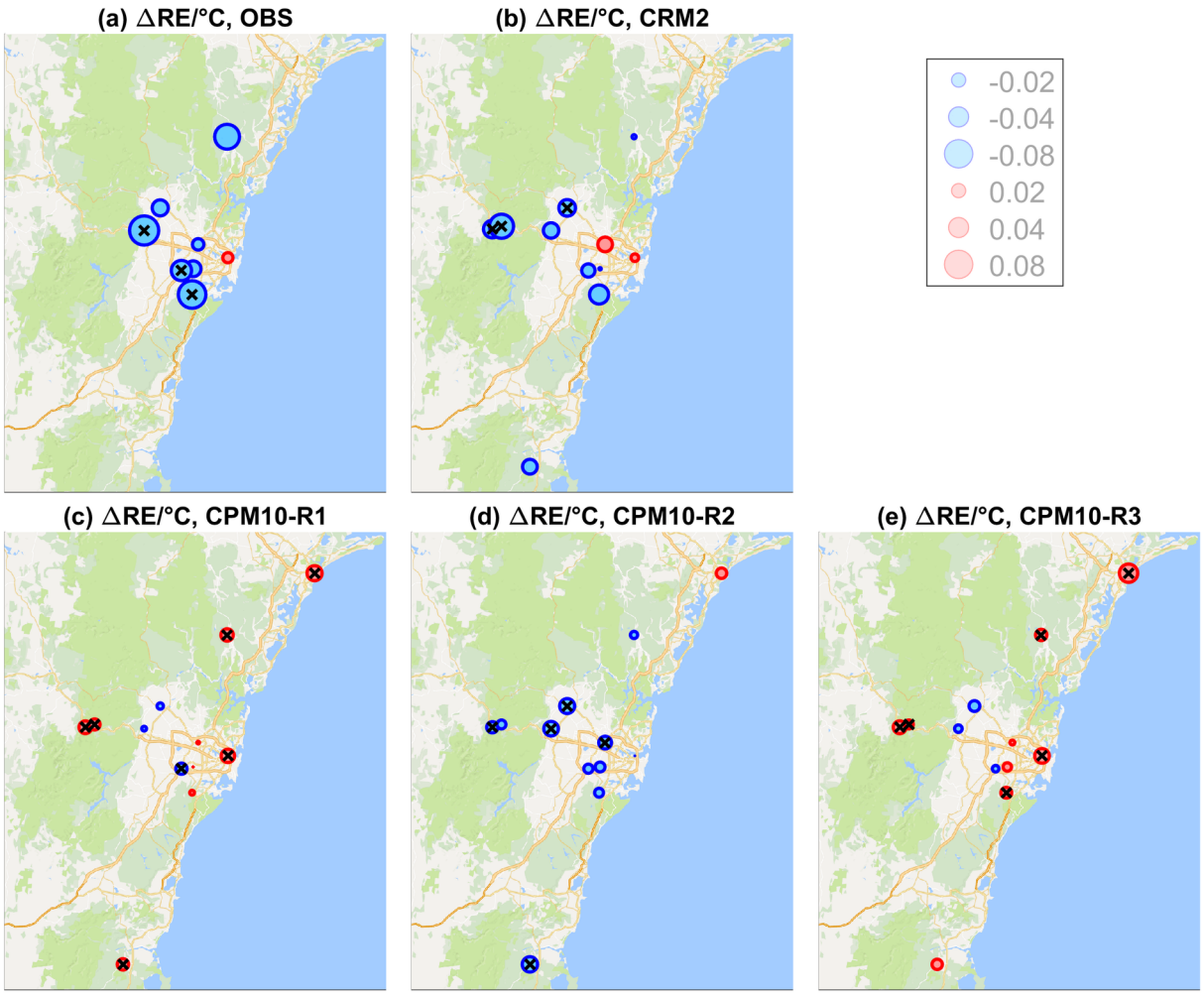

2018GL077716-f03-z-.tif

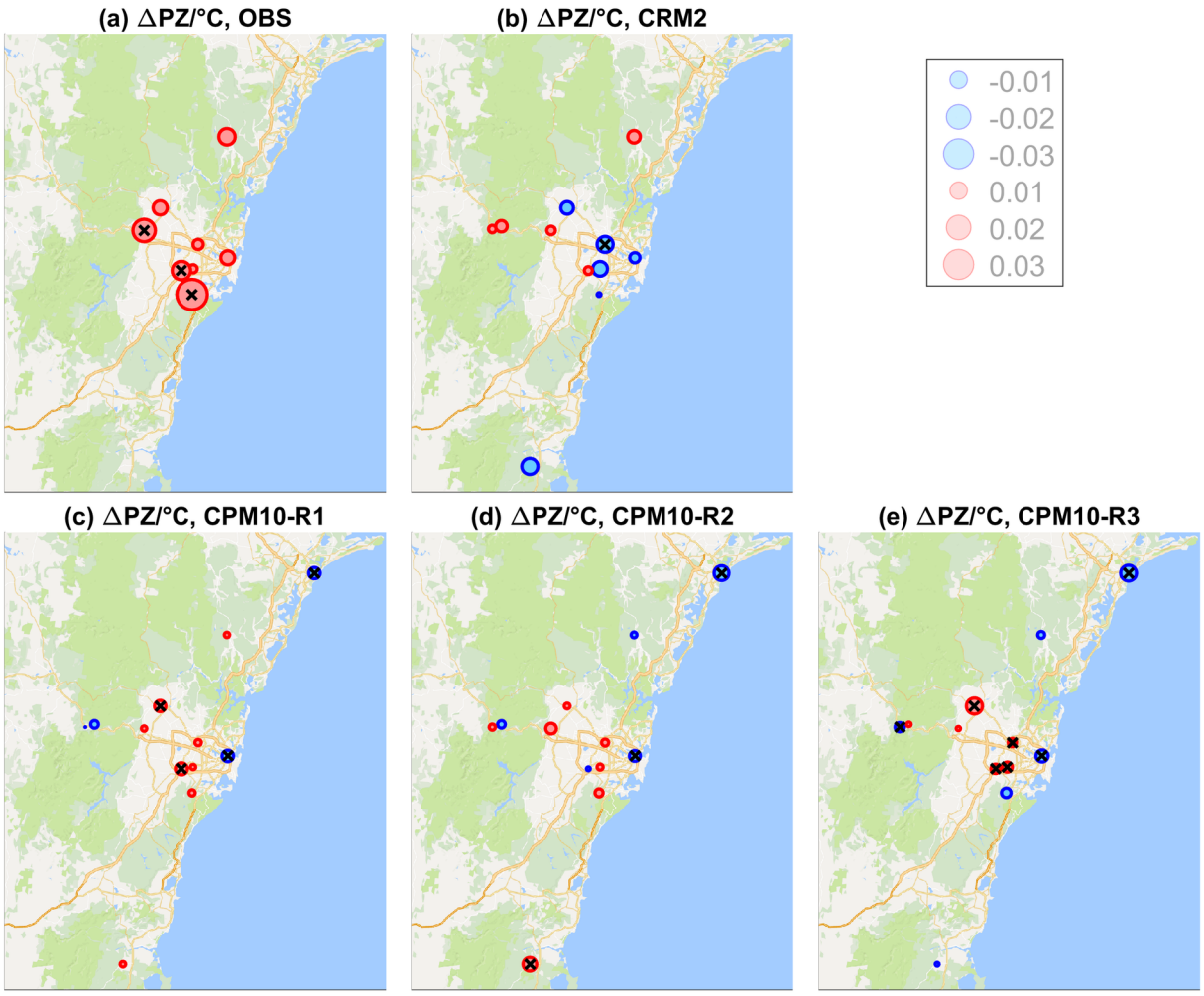

2018GL077716-f04-z-.tif

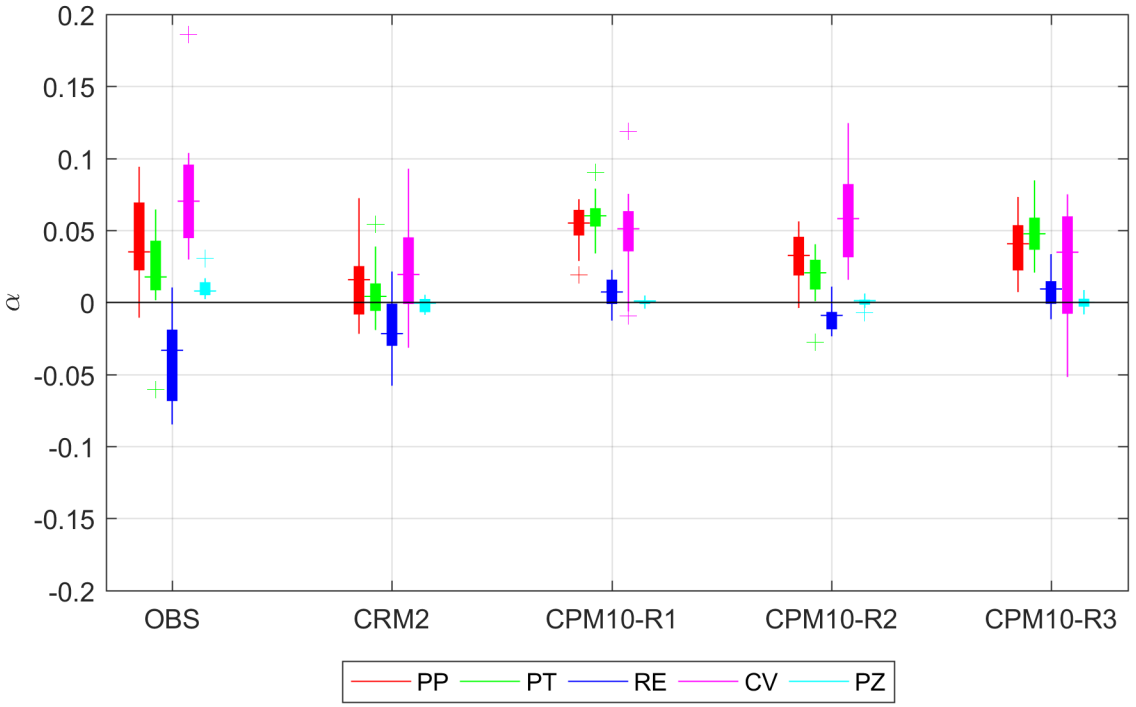

2018GL077716-f05-z-.tif